Stem Cell Reports
Article

ISSCR

OPEN ACCESS

MSC-derived Extracellular Vesicles Attenuate Immune Responses in Two Autoimmune Murine Models: Type 1 Diabetes and Uveoretinitis

Taeko Shigemoto-Kuroda,[1,5] Joo Youn Oh,[2,3,5] Dong-ki Kim,[1] Hyun Jeong Jeong,[3] Se Yeon Park,[3] Hyun Ju Lee,[3] Jong Woo Park,[3] Tae Wan Kim,[4] Su Yeon An,[1] Darwin J. Prockop,[1] and Ryang Hwa Lee[1,*]

[1]Institute for Regenerative Medicine, College of Medicine, Texas A&M University, 1114 TAMU, 206 Olsen Boulevard, College Station, TX 77845, USA
[2]Department of Ophthalmology, Seoul National University Hospital, 101 Daehak-ro, Jongno-gu, Seoul 110-744, Korea
[3]Laboratory of Ocular Regenerative Medicine and Immunology, Biomedical Research Institute, Seoul National University Hospital, 101 Daehak-ro, Jongno-gu, Seoul 110-744, Korea
[4]Department of Ophthalmology, Seoul National University Boramae Medical Center, Seoul 07061, Korea
[5]Co-first author
*Correspondence: rlee@medicine.tamhsc.edu
http://dx.doi.org/10.1016/j.stemcr.2017.04.008

SUMMARY

Accumulating evidence shows that extracellular vesicles (EVs) produced by mesenchymal stem/stromal cells (MSCs) exert their therapeutic effects in several disease models. We previously demonstrated that MSCs suppress autoimmunity in models of type 1 diabetes (T1D) and experimental autoimmune uveoretinitis (EAU). Therefore, here, we investigated the therapeutic potential of MSC-derived EVs using our established mouse models for autoimmune diseases affecting the pancreas and the eye: T1D and EAU. The data demonstrate that MSC-derived EVs effectively prevent the onset of disease in both T1D and EAU. In addition, the mixed lymphocyte reaction assay with MSC-derived EVs indicated that EVs inhibit activation of antigen-presenting cells and suppress development of T helper 1 (Th1) and Th17 cells. These results raise the possibility that MSC-derived EVs may be an alternative to cell therapy for autoimmune disease prevention.

INTRODUCTION

Mesenchymal stem/stromal cell (MSC)-based therapeutic intervention has become an emerging strategy for immune modulation, and therefore MSCs have been exploited in a variety of clinical trials for immune-mediated disorders, including autoimmune diseases. Although the exact mechanisms underlying the immunomodulatory functions of MSCs remain largely unknown, MSCs have shown suppressive effects on many types of immune cells in vitro and in vivo. For example, it has been demonstrated that MSCs directly suppress T cell activation/proliferation and induce T cell apoptosis by expressing nitric oxide (NO), indoleamine 2,3, dioxygenase (IDO), programmed death ligand 1 (PD-L1), or Fas ligand (Abdi et al., 2008; Akiyama et al., 2012; Jurewicz et al., 2010; Lee et al., 2011; Lenardo et al., 1999; Meisel et al., 2004; Sato et al., 2007; Wei et al., 2013). Also, MSCs have been shown to affect differentiation, maturation, and function of antigen-presenting cells (APCs), including dendritic cells (DCs) and macrophages, which results in conversion of APCs into a suppressive or tolerogenic phenotype (Aldinucci et al., 2010; Beyth et al., 2005; Chiesa et al., 2011; Jiang et al., 2005; Kronsteiner et al., 2011; Liu et al., 2013; Spaggiari et al., 2009; Zhang et al., 2004, 2009).

Although MSC therapies are safe compared with embryonic stem cells or induced pluripotent stem cells, which have tumorigenic potential, there are still concerns that MSCs might trigger tumorigenicity, allo-immune responses, and pulmonary embolism in a clinical setting (Ankrum et al., 2014; Barkholt et al., 2013; Boltze et al., 2015; Heslop et al., 2015; Isakova et al., 2014; Jung et al., 2013). In line with these clinical findings, we and others observed that intravenous administration of MSCs caused embolism and death in several mice (Furlani et al., 2009; Lee et al., 2009b; Tatsumi et al., 2013). Therefore, the long-term safety of MSC administration in human patients requires further investigation.

Accumulating evidence indicates that treatment using extracellular vesicles (EVs) have multiple advantages over cell therapy, because EVs are stable in the circulation without losing function and exhibit a superior safety profile (Vader et al., 2016). In particular, MSCs are an attractive source of EVs because they secrete a large number of therapeutic factors, including cytokines, chemokines, and microRNAs in EVs (Aggarwal and Pittenger, 2005; Baglio et al., 2015; Jurewicz et al., 2010; Lee et al., 2011; Meisel et al., 2004; Phinney et al., 2015; Rafei et al., 2008; Sato et al., 2007; Wei et al., 2013). In addition, since MSCs have a remarkable tendency to home to injured tissues (Kidd et al., 2009; Ortiz et al., 2003; Rojas et al., 2005), the EVs produced by MSCs may retain the homing properties of their parent cells (Hood et al., 2011; Lai et al., 2013). Indeed, a number of studies have shown that EVs produced by MSCs exert their therapeutic effects in several disease models (Chen et al., 2015; Doeppner et al., 2015; Heldring et al., 2015; Monsel et al., 2016; Ophelders et al., 2016; Rani et al., 2015; Vader et al., 2016; Wen et al., 2016), suggesting

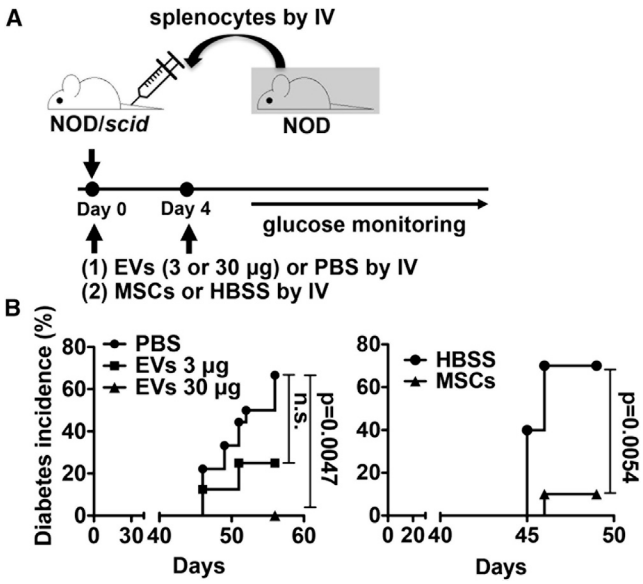

Figure 1. MSCs and MSC-derived EVs Delay the Onset of T1D in Mice

(A) Experimental scheme. On day 0, MSCs (1×10^6 cells), EVs (3 μg or 30 μg), or vehicle control were intravenously (IV) infused immediately after injection of splenocytes from diabetic NOD mice into NOD/*scid* mice. On day 4, MSCs, EVs, or vehicle control were infused again. Mice were monitored for hyperglycemia.

(B) Diabetes incidence. PBS (n = 18); 3 μg EVs (n = 8); 30 μg EVs (n = 10); HBSS (n = 10); MSCs (n = 10). p Value by Kaplan-Meier estimator.

that MSC-derived EVs may be a promising alternative to cell therapy for immune-mediated diseases.

Our group has previously demonstrated that MSCs induce immune tolerance by activating the endogenous immune regulatory system of the recipients and thereby suppress autoimmune responses in models of type 1 diabetes (T1D) (Kota et al., 2013) and experimental autoimmune uveoretinitis (EAU) (Ko et al., 2016; Lee et al., 2015; Oh et al., 2014). Therefore, here, we investigated whether MSC-derived EVs are as effective in modulating immune responses as MSCs in two models for autoimmune diseases: T1D and EAU.

RESULTS

MSC-Derived EVs Delay the Onset of T1D in Mice

Since we have previously shown immunosuppressive capacity of MSCs in T1D, we tested whether EVs produced by MSCs reproduce immune modulatory effects in mice with T1D. To induce an adoptive transfer T1D model, we intravenously infused splenocytes isolated from 12-week-old female NOD mice into 7-week-old female NOD/*scid* mice (Figure 1A). To test the effects of MSC-derived EVs, we injected either (1) MSC-derived EVs (3 μg or 30 μg containing 15×10^8 or 15×10^9 EVs per mouse) or their vehicle control (PBS) or (2) MSCs (1×10^6 cells per mouse, donor #6015, the same lot of MSCs from which the EVs were produced) or their vehicle control (Hank's balanced salt solution [HBSS]) into the tail vein right after adoptive splenocyte transfer. Mice received an additional treatment at day 4 as shown in Figure 1A. Recipient NOD/*scid* mice were monitored for hyperglycemia twice a week, and development of diabetes was defined as the mouse having a glycemic value >250 mg/dL. As shown in Figure 1B, both MSC-derived EVs and MSCs significantly delayed the onset of T1D in an adoptive transfer T1D model. Histologic analysis revealed that most of the islets were already destroyed at day 58, and the remaining islets showed severe insulitis in the PBS-treated mice (Figures 2A, 2B, and 2D). In contrast, administration of MSC-derived EVs or MSCs suppressed insulitis and preserved insulin-producing cells in the islets (Figures 2A, 2B, and 2D). In addition, there were fewer $CD4^+$ cells in islets of EV- or MSC-treated mice, while $CD4^+$ cells were present in significant numbers in the PBS-treated mouse islets (Figure 2D). Consistent with these histologic results, the plasma levels of insulin were significantly increased by treatment with either EVs or MSCs (Figure 2C). These results demonstrated that MSC-derived EVs were as effective in delaying the onset of T1D in mice as MSCs.

MSC-Derived EVs Prevent Development of EAU

In parallel experiments, we tested the effects of MSC-derived EVs in a mouse model of EAU (Ko et al., 2016), a well-established model for human autoimmune intraocular inflammation, and compared them with the effects of MSCs. Immediately after EAU immunization (day 0), we administered (1) MSC-derived EVs (30 μg containing 15×10^9 EVs per mouse), (2) MSCs (1×10^6 cells per mouse, donor #6015, the same lot of MSCs from which EVs were produced), or (3) their vehicle control (PBS) through tail-vein injection (Figure 3A). The mice were killed on day 21, and the eyes and cervical draining lymph nodes (CLNs) were assayed. We selected to use day 21 for evaluation because in previous time-course experiments, we found that both retinal destruction and T helper 1 (Th1)/Th17 activation in CLNs were at their peak (Figure S1). Retinal cross-sections on day 21 showed severe disruption of the retinal photoreceptor layer and infiltration of inflammatory cells, including $CD3^+$ T cells in the retina and vitreous cavity in EAU mice treated with PBS (Figures 3B and 3C). In contrast, there was little structural damage with few inflammatory infiltrates in the eyes of EAU mice that received MSCs or MSC-derived EVs, similar to the normal retina without

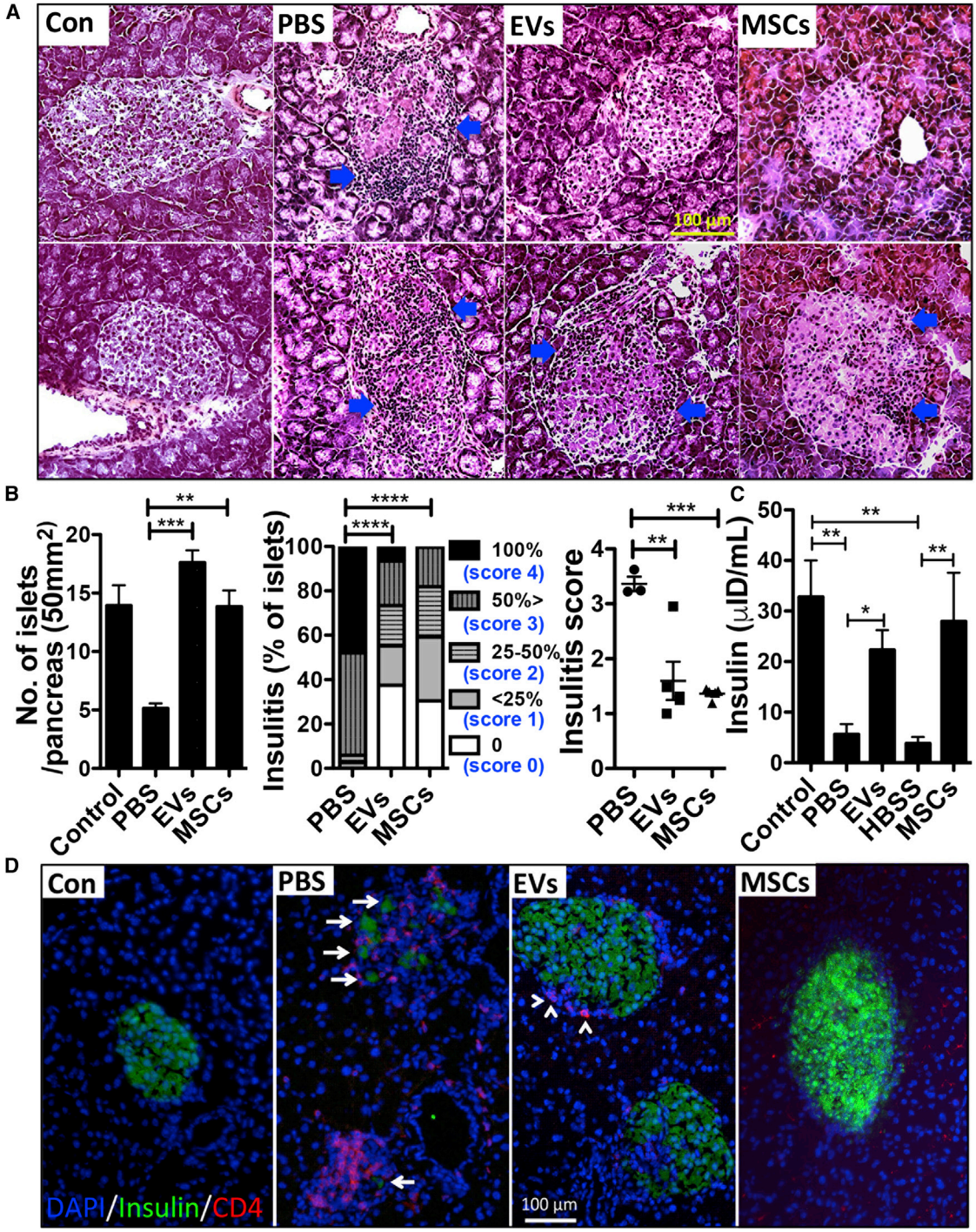

Figure 2. MSC-derived EVs Suppress Insulitis in Islets

(A) The animals from Figure 1B were killed on day 58 (EV-treated group) and day 50 (MSC-treated group) for tissue harvesting and blood collection, respectively. Representative H&E staining of the pancreases. Arrows indicate islet-infiltrating immune cells. The control pancreas (Con) was obtained from age-matched NOD/*scid* mice.

(B) Number of islets in the pancreas per slide (50 mm^2; the bar represents the mean + SD; $^{**}p < 0.01$, $^{***}p < 0.001$ by one-way ANOVA with Dunnett's Multiple Comparison Test), the percentage of islets in each of the infiltration categories (no insulitis, score 0; peri-insular [<25%], score 1; 25–50% islets infiltrated, score 2; >50% islet infiltrated, score 3; 100% islet infiltrated, score 4) ($^{****}p < 0.0001$ by

(legend continued on next page)

EAU induction (Figure 3B). The disease score assigned by retinal pathology was significantly lower in MSC- or MSC-derived EV-treated mice compared with the PBS-treated mice (Figure 3B). Also, the number of $CD3^+$ T cells infiltrating the retina was significantly reduced by either MSCs or MSC-derived EVs (Figure 3C). There were no differences in the disease score and the number of infiltrating $CD3^+$ cells between MSC-derived EV- and MSC-treated groups.

Similarly, the transcript levels of pro-inflammatory cytokines, interferon gamma (IFN-γ), interleukin (IL)-17A, IL-2, IL-1β, IL-6, and IL-12A were significantly lower in the eyes of mice in the MSC- or MSC-derived EV-treated group compared with the PBS-treated controls (Figure 4A). However, the mRNA levels of IL-4 and IL-10 were not affected by the treatment (Figure 4A). The effects of MSC-derived EVs in the reduction of inflammatory markers were comparable with those of MSCs. In addition, flow cytometric assays of CLNs revealed that the number of IFN-γ^+CD4^+ cells and IL-17^+CD4^+ cells was significantly lower in MSC- or MSC-derived EV-treated mice than in the PBS-treated mice (Figure 4B). The number of $FOXP3^+$ regulatory T cells (Tregs) was not different in all groups (Figure S2). Together, these data indicate that MSC-derived EVs are as effective in suppressing Th1 and Th17 cells and preventing the development of EAU as their parent cells.

MSC-Derived EVs Suppress T Cell Proliferation in Allogeneic Mixed Lymphocyte Reaction

To understand the underlying mechanism of MSC-derived EVs in modulating the immune response, we next examined the effects of MSC-derived EVs on immune-cell activation using allogeneic mixed lymphocyte reaction (MLR) assays. Consistent with our previous observation with MSCs (Kota et al., 2013), MSC-derived EVs significantly reduced the production of IFN-γ, IL-12 p70, and tumor necrosis factor alpha (TNF-α) in the MLR (Figure 5A), suggesting that MSC-derived EVs suppress Th1 development. In addition, MSC-derived EVs significantly suppressed production of IL-6, a key cytokine for the lineage commitment of pathogenic IL-17 producing Th17 cells (Kimura et al., 2007), as well as IL-17 in the MLR, indicating that MSC-derived EVs also suppress Th17 development (Figure 5B). We further examined whether the MSC-derived EVs suppress Th1 and Th17 development by inducing Tregs. However, there was no increase in $FOXP3^+$ Tregs on day 6 of the MLR (Figure 5C) and IL-10, a cytokine that induces Tregs, on day 5 of the MLR (Figure 5D), indicating that the EVs suppressed T cell proliferation by directly inhibiting Th1 and Th17 development, not by inducing Tregs.

MSC-Derived EVs Suppress Activation of APCs and T Cells

To investigate the effects of EVs on APC activation, we examined the expression of costimulatory factors (CD80, CD86, and CD40) and major histocompatibility complex (MHC) class II in APCs cultured in the presence of EVs. The results showed that EV treatment suppressed the expression of costimulatory factors and MHC class II in $CD11c^+$ cells on day 2 of the MLR in a dose-dependent manner (Figures 6A, 6B, and 6C). Also, the MSC-derived EV treatment significantly increased the levels of IL-10 on day 2 of the MLR (Figure 6D). To examine whether EVs directly suppress APC activation, we repeated the MLR with whole splenocytes isolated from BALB/c mice as stimulator cells and only $CD11c^+$ cells isolated from C57BL/6 mouse splenocytes as responder cells. As shown in Figure 6E, EV treatment still suppressed the expression of costimulatory factors and MHC class II in $CD11c^+$ cells. These data suggest that APCs exhibit a hypoactive phenotype, including the suppressed allorecognition, and thereby suppress subsequent T cell proliferation in the MLR. To further examine whether the EVs also directly inhibit T cell activation, we isolated $CD4^+$ T cells from mouse splenocytes and stimulated them with CD3/CD28 beads. The results showed that EV treatment also suppressed T cell activation as indicated by decreased levels of IL-2 and IFN-γ (Figure 6F). Together, these data suggest that the EVs suppress activation of both APCs and T cells in the MLR.

DISCUSSION

Here, we demonstrate the therapeutic potential of MSC-derived EVs in two mouse models of autoimmune diseases involving the pancreas and the eye. Consistent with our previous observations with MSCs (Ko et al., 2016; Kota et al., 2013), MSC-derived EVs suppressed Th1 development and inhibited activation of APCs and T cells. In addition, they also increased expression of the immunosuppressive cytokine IL-10 and suppressed Th17

two-way ANOVA) and insulitis scores (**p < 0.01; ***p < 0.001 by one-way ANOVA). Five slides per mouse (three or five mice per group) were analyzed.

(C) Expression of insulin in the plasma. The bar represents the mean + SD. *p < 0.05, **p < 0.01 by one-way ANOVA with Tukey's multiple comparison test.

(D) Representative immunofluorescence staining for insulin (green) and CD4 (red). Nuclei were counterstained with DAPI (blue). Arrows indicate expression of insulin and arrowheads indicate CD4 signals. Scale bar, 100 μm.

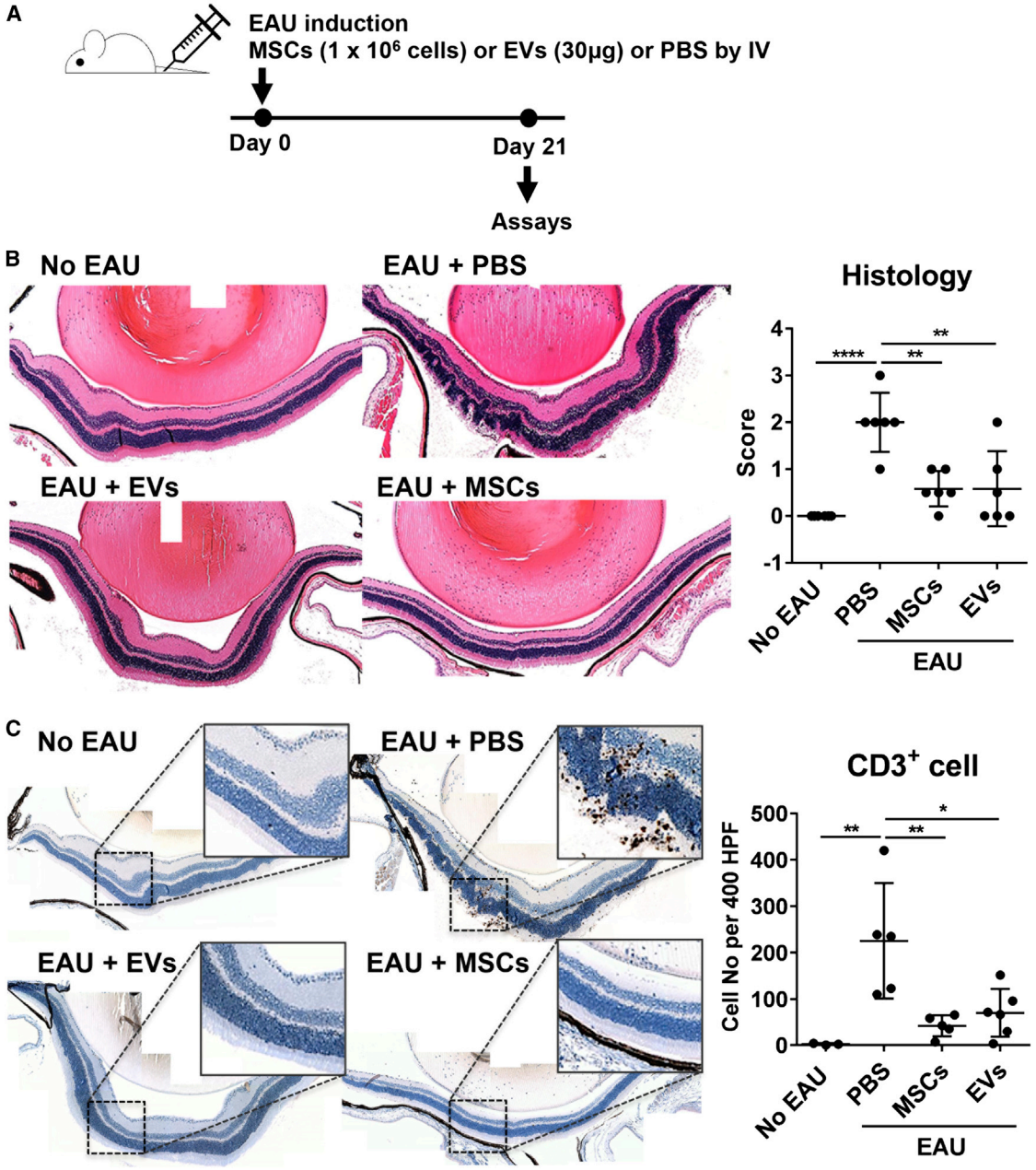

Figure 3. MSCs and MSC-derived EVs Prevent Development of EAU in Mice

(A) Experimental scheme. On day 0, EAU was induced by subcutaneous IRBP injection and intraperitoneal pertussis toxin injection. Right after induction, either MSCs (1×10^6 cells) or MSC-derived EVs (30 μg containing 15×10^9 EVs) were injected into the tail vein. As a control, the same volume of PBS was injected. On day 21, the eyeballs and draining cervical lymph nodes were collected for assays.

(B) Representative microphotographs of H&E staining of the eyes (100× magnification), and histologic disease scores of retinal pathology.

(C) Representative microphotographs of CD3 immunostaining of the eyes (100× magnification), and quantitative data of the number of $CD3^+$ cells infiltrating the retina and vitreous cavity.

Dots represent a single animal, and the data are presented as means ± SD. *$p < 0.05$, **$p < 0.01$, ****$p < 0.0001$ by one-way ANOVA.

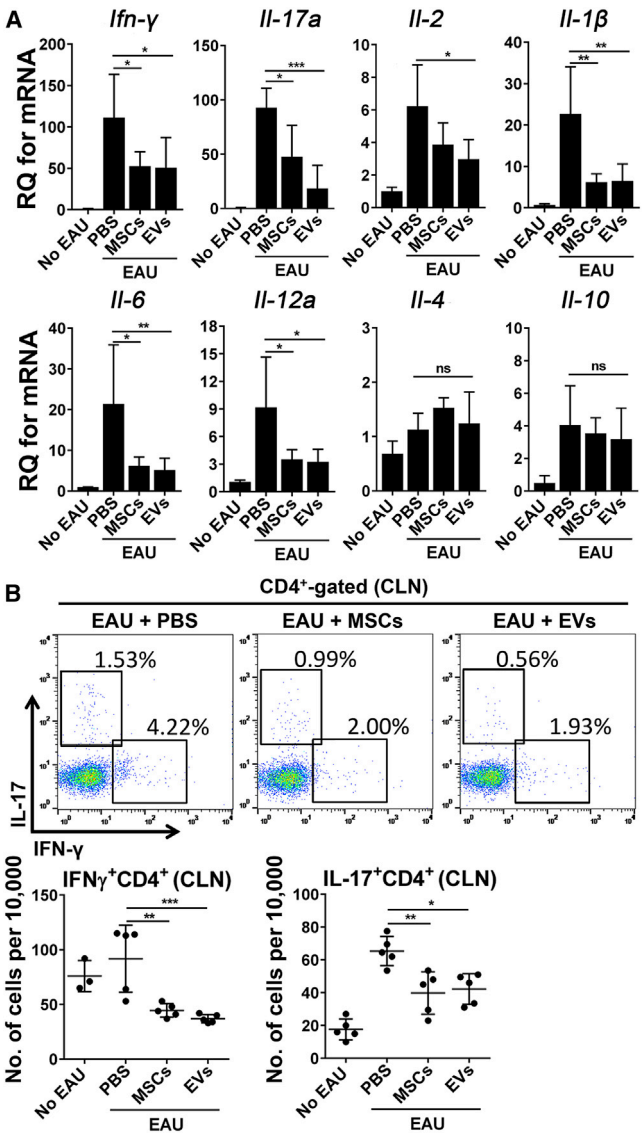

Figure 4. MSC-Derived EVs Suppress Th1 and Th17 Development in EAU Mice

(A) Relative quantification (RQ) of Th1 and Th17 cytokines in the eyes of the animals from Figure 3A with real-time RT-PCR assays. Data (mean + SD) were obtained from six mice per group.

(B) Representative flow cytometry plots and quantitative results for Th1 and Th17 cells in cervical lymph nodes (CLNs) collected from animals as in Figure 3A. Dots indicate a single animal in (B).

The bar represents the mean ± SD. *p < 0.05, **p < 0.01, ***p < 0.001 by one-way ANOVA.

cell development. IL-10 has been considered an immunosuppressive cytokine because of its association with multiple suppressive immune-cell populations, such as Tregs and regulatory DCs, as well as its inhibition of antigen presentation and immune-cell activation (Ouyang et al., 2011; Zhang et al., 2016). Given our results of increased IL-10 and the hypoactive phenotype of DCs at the early time point of the MLR (day 2), MSC-derived EVs might induce IL-10-expressing regulatory DCs, and thereby, regulatory DCs subsequently suppress Th1 and Th17 cell development without inducing Tregs. Furthermore, Th1 cytokine production is characteristic of many organ-specific autoimmune diseases (Alleva et al., 2001; Crane and Forrester, 2005; Jun et al., 1999; Weaver et al., 2001), and IL-17A and/or IL-17F are responsible for development of inflammation in many disorders, especially in autoimmune diseases (Bettelli et al., 2007; Jain et al., 2008; Langrish et al., 2005; Nakae et al., 2002). Therefore, our data raise the possibility that MSC-derived EVs might be beneficial for treating autoimmune diseases where Th1 and Th17 cells play a critical role.

The immunosuppressive effect of MSCs is mediated by a range of immunosuppressive mediators such as NO, IDO, prostaglandin E2 (PGE2), TNF-α-simulated gene 6 (TSG-6), CCL-2, or PD-L1 (Aggarwal and Pittenger, 2005; Jurewicz et al., 2010; Lee et al., 2011; Meisel et al., 2004; Rafei et al., 2008; Sato et al., 2007; Wei et al., 2013). Since MSCs need to be activated to increase the expression of these therapeutic factors by inflammatory cytokines such as TNF-α or IFN-γ (Lee et al., 2009a; Wei et al., 2013), EVs isolated from unactivated MSCs are likely to express lower levels of therapeutic factors. To obtain EVs for our study, we incubated MSCs in a chemically defined protein-free medium, which activates MSCs to increase therapeutic proteins, including TSG-6, and also provides a stable environment for producing EVs (Kim et al., 2016). Therefore, the EVs produced in our study might have advantages over the EVs produced by unactivated MSCs. Moreover, MSCs cultured in serum-free media would be ideal for a clinical-grade therapeutic product.

However, there are still some challenges that need to be addressed in order for our findings to be developed as an effective treatment for autoimmunity prevention. First, although islet function was preserved in the EV-treated mice, decreased β cell mass in association with insulitis was still observed in the EV-treated mice as shown in Figures 2A and 2B, suggesting that further study is needed to optimize the injection frequency and dose to maintain the long-lasting immunomodulation effects of EVs. Furthermore, the main problem with MSC-derived EV-based therapy is that EVs are highly heterogeneous, depending on the cellular source, state, and environmental conditions. Our previous study showed that MSCs isolated from different donors exhibit huge variation in their therapeutic efficacy in suppressing inflammation in vivo, and some MSCs even fail to show any therapeutic effects in sterile inflammation-mediated disease models (Lee et al., 2014). But, we found that

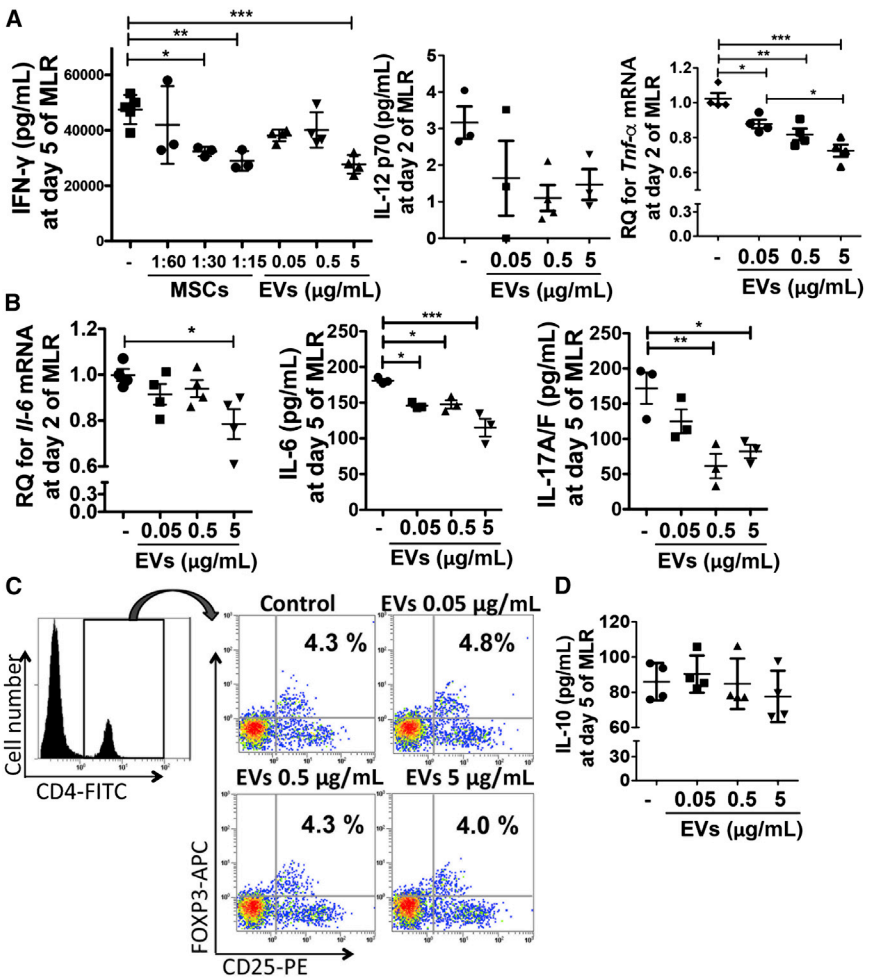

Figure 5. MSC-Derived EVs Suppress Th1 and Th17 Development in the MLR

(A) Splenic Th1 cytokine expressions at day 5 (IFN-γ; n = 3 for MSCs and n = 4 for EVs) and day 2 (IL-12 p70; n = 3 and TNF-α; n = 4) in the MLR with or without MSCs or MSC-derived EVs. Ratio of MSCs to splenocytes = 1:15, 1: 30, and 1: 60.

(B) Th17 cytokine expression at day 2 (IL-6; n = 4) and day 5 (IL-6 and IL-17A/F; n = 3) in the MLR with or without MSC-derived EVs.

(C) Representative flow cytometry plots of $CD4^+CD25^+FOXP3^+$ cells in the MLR assay with or without MSC-derived EV treatment. The cells were first gated on CD4 expression and further analyzed for the expression of CD25 and FOXP3.

(D) Expression of IL-10 at day 5 in the MLR with or without MSC-derived EVs (n = 4).

Dots indicate independent experiments and all values are means ± SD. *p < 0.05, **p < 0.01, ***p < 0.001 by one-way ANOVA.

the therapeutic efficacy of MSCs in suppressing sterile inflammation correlates with the TSG-6 mRNA level in MSCs (Lee et al., 2014). Therefore, we selected MSCs expressing a high level of TSG-6 to prepare EVs for the current study, considering the marked donor variation of their therapeutic efficacy in vivo. However, further study is needed to investigate whether therapeutic efficacy of MSC-derived EVs correlates with their parent cells, and the TSG-6 level in MSCs can also be used as a biomarker to select the cell source for EV production. Hence, pre-selecting the most effective cellular source for EV production will help to avoid variation in the therapeutic efficacy of MSC-derived EVs and is essential for successful clinical translation. Lastly, defining the therapeutic factors responsible for the immunomodulation effect in EVs will also help to develop a biomarker to select the effective cellular source for EV preparation and provide a strategy to maximize their therapeutic efficacy, for example, by manipulating the cellular source of EVs by overexpressing the defined therapeutic factors.

In conclusion, our study shows that MSC-derived EVs have significant potential as an alternative to cell therapy for autoimmune diseases prevention.

EXPERIMENTAL PROCEDURES

MSC Culture and Isolation of MSC-Derived EVs

Human MSCs (donor #6015) were prepared as previously described (Lee et al., 2009a) and EVs derived from MSCs were prepared as previously described (Kim et al., 2016). In brief, a frozen vial of passage 3 to 4 MSCs was plated directly at about 200–500 cells per cm^2 in tissue culture plates in complete culture medium (CCM). CCM was replaced after 2–3 days. After the cells reached about 70% confluency in 4–6 days, the MSCs were either harvested for mouse injections or incubated with a medium optimized for Chinese hamster ovary cells (CD-CHO Medium; Invitrogen; Thermo Fisher Scientific) with additional supplements (Kim et al., 2016) for EV production. After 6 hr, the medium was discarded and replaced by fresh medium and recovered at 48 hr to isolate EVs. For isolation of EVs, the medium was centrifuged at 2,565 × *g* for 15 min to

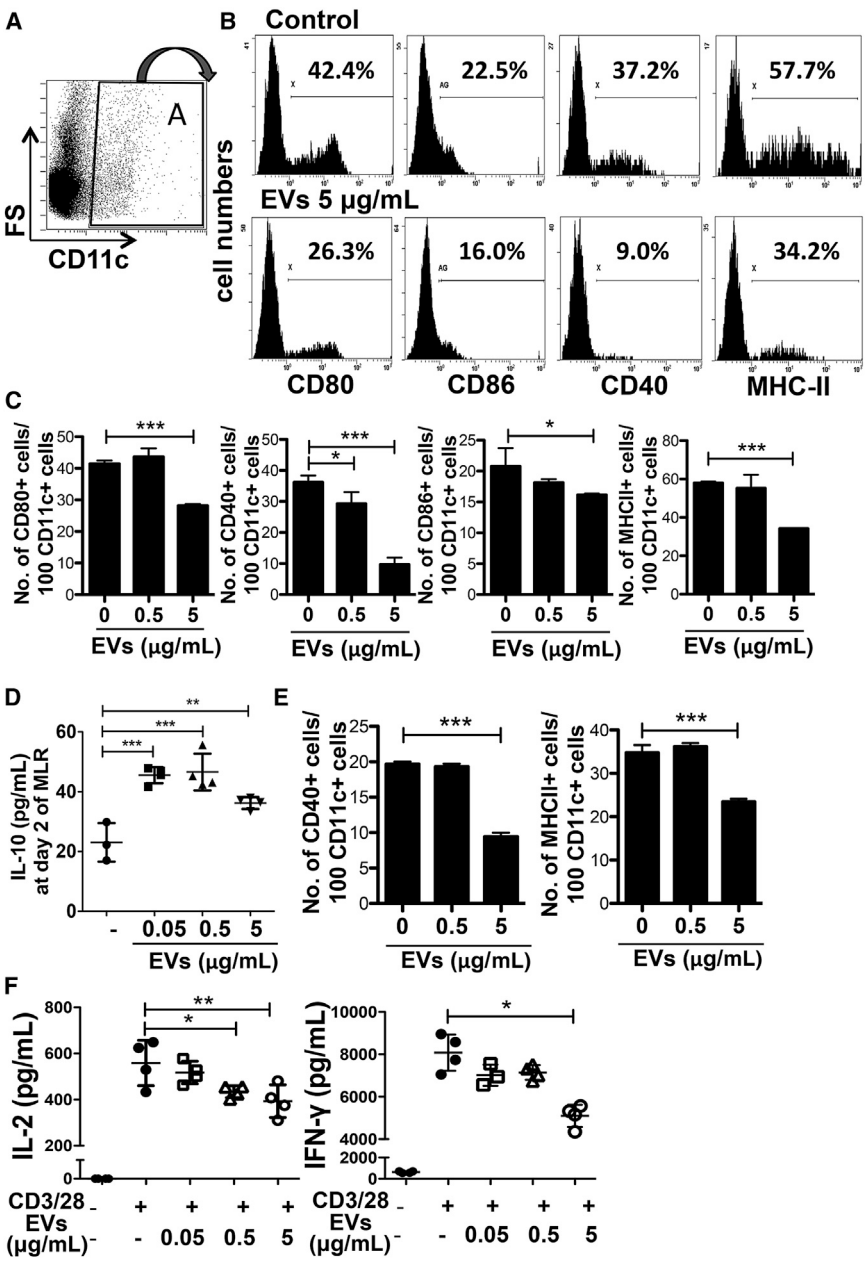

Figure 6. MSC-Derived EVs Suppress Activation of APCs and T Cells in the MLR

(A–C) Representative flow cytometry plots (A and B) and quantification (C) of CD80, CD86, CD40, and MHC-class-II-positive cells in $CD11c^+$ cells on day 2 of the MLR assay with or without MSC-derived EV treatment. The cells were first gated on CD11c expression, and further analyzed for the expression of CD80, CD86, CD40, and MHC class II (n = 3).

(D) Expression of IL-10 at day 2 in the MLR with or without MSC-derived EVs (n = 3 for control; n = 4 for EVs).

(E) Quantification of flow cytometry analysis of CD40, and MHC-class-II-positive cells in $CD11c^+$ cells on day 2 of the MLR assay with $CD11c^+$ responder cells (n = 3).

(F) Expression of IL-2 and IFN-γ in CD4-positive cells at day 2 upon CD3/28 bead stimulation (n = 4).

Dots indicate independent experiments and all values are means ± SD. *p < 0.05, **p < 0.01, ***p < 0.001 by one-way ANOVA.

remove cellular debris, and the supernatant was applied directly at room temperature to a column containing anion exchange resin (Express Q; cat. no. 4079302; Whatman; 100-mL bed volume) that had been equilibrated with 50 mM NaCl in 50 mM Tris buffer (pH 8.0). The medium was applied at a flow rate of 4 mL/min and at room temperature. The column resin was washed with 10 volumes of the equilibration buffer and then eluted with 25 volumes of 500 mM NaCl in 50 mM Tris buffer (pH 8.0). Fractions of 20–30 mL were collected and stored at −80°C before the in vitro and in vivo assays. The EVs in the peak fractions were positive for the exosome markers, CD63 and CD81, but negative for 11 other epitopes found on the MSCs from which they were recovered (Kim et al., 2016). Also, they were about 100 nm in diameter (Kim et al., 2016).

Adoptive Transfer T1D Mouse Model

Female NOD/LtJ (12 weeks old) and female NOD/*scid* mice (7 weeks old) were used for the adoptive transfer model. All mice were purchased from Jackson Laboratory and cared for at the Scott & White Department of Comparative Medicine under a protocol approved by the Institutional Animal Care and Use Committee. To induce an adoptive transfer in the T1D model, 1×10^7 splenocytes from pre-diabetic 12-week-old female NOD mice were intravenously

injected into 7-week-old female NOD/*scid* mice. MSCs (1×10^6, #6015, the same lot of MSCs from which the EVs were produced), EVs (15×10^9 or 30 μg), or vehicle control were injected intravenously twice at 15 min and on day 4 after splenocyte transfer. Blood glucose levels were measured twice a week by tail bleeding according to NIH guidelines, and diabetes in mice was defined as having the two consecutive glycemic values above 250 mg/dL.

Pancreas Histologic Analysis after Adaptive Transfer in the T1D Model

Serial pancreatic sections (5 μm) were prepared from at least three mice per group. Every 20th section (n = 5) was stained with H&E, and the islet number per section (about 50 mm^2 area) was quantified. Insulitis scoring was performed on H&E-stained pancreatic sections as we have shown previously (Kota et al., 2013). Briefly, insulitis was scored as follows: score 0, normal islets; score 1, mild mononuclear infiltration (<25%) at the periphery; score 2, 25%–50% of the islets infiltrated; score 3, >50% of the islets infiltrated; score 4, islets completely infiltrated with no residual parenchyma remaining. The insulitis scores were presented as the proportion of islets in each scoring category and means as shown previously (Wang et al., 2005). For immunofluorescence, the sections were incubated for 18 hr at 4°C with antibodies against mouse insulin (1:100, clone C27C9; catalog no. 3014; Cell Signaling Technology) and mouse CD4 (1:100, YTS191.1; catalog no. MCA1767; Bio-Rad Laboratories).

EAU Mouse Model

The experimental protocols were approved by the Institutional Animal Care and Use Committee of Seoul National University Biomedical Research Institute (IACUC No. 13-0104-C1A1). Six-week-old female B6 mice (C57BL/6J, H-2b; Orient Bio) were immunized by subcutaneous injection into a footpad of the retina-specific antigen, interphotoreceptor retinal binding protein (IRBP) peptide 1–20, GPTHLFQPSLVLDMAKVLLD (250 μg; Peptron) emulsified in complete Freund adjuvant (Sigma-Aldrich) containing *Mycobacterium tuberculosis* (2.5 mg/mL; BD Difco). Simultaneously, the mice received an intraperitoneal injection of 0.7 μg pertussis toxin (300 μL; Sigma-Aldrich). Immediately after immunization, MSC-derived EVs (15×10^9 or 30 μg of EVs) in 150 μL of PBS, 1×10^6 MSCs (#6015, the same lot of MSCs from which EVs were produced) in 150 μL of PBS, or the same volume of PBS were injected via tail vein into the mice.

Eyeball Histology

Twenty-one days later, the mice were killed and the eyeballs were collected for the assays. Eyeballs were subjected to histologic and molecular assays. For histology, the eyeballs were fixed in 10% formaldehyde and embedded in paraffin. Serial 4 μm thick sections were cut and stained with H&E and CD3 immunohistochemical staining. For CD3 immunohistochemical staining, a rabbit anti-mouse CD3 (catalog no. ab5690; Abcam) was used as a primary antibody. The pathologic features of the retina were examined, and histologic disease score was assessed by two independent observers (J.Y.O. and T.W.K.) in a blinded manner on a scale of 0–4 using the criteria defined previously by Caspi (2003). The number of CD3-stained cells was calculated under a microscope using a ×20 objective.

Allogeneic Mixed Lymphocyte Reaction

MSCs or EVs were co-cultured in 96-well plates with splenocytes from BALB/c mice (0.3 M cells/well) and C57BL/6 mice (0.6 M cells/well) in 5% heat-inactivated FBS (Atlanta Biologicals) plus 100 units/mL penicillin and 100 mg/mL streptomycin (pen/strep; both from Life Technologies) in RPMI-1640 medium (ATCC). All mice were purchased from Jackson Laboratory. MSCs and splenocytes from BALB/c mice were pretreated with mitomycin (2.5 mg/mL for 2 hr at 37°C; Sigma-Aldrich) before co-culture. Two days or five days later, mouse cytokine expression was measured by real-time PCR assays or ELISAs according to the manufacturer's protocols.

Isolation and Activation of T Cells

$CD4^+$ T cells were isolated from splenocytes from BALB/c mice by a $CD4^+$ T Cell Isolation Kit II (Miltenyi Biotec) according to the manufacturer's protocol. The $CD4^+$ T cells were cultured in 96-well plates with CD3/CD28 beads (Life Technologies) with or without EVs in RPMI-1640 medium containing 5% heat-inactivated FBS, 100 units/mL penicillin, and 100 mg/mL streptomycin. Two days later, the levels of Th1 cytokines were detected by ELISA according to the manufacturer's protocols.

Flow Cytometry Analysis

CLNs from mice were analyzed for Th1, Th17, and Tregs by flow cytometry at 21 days after EAU induction. For flow cytometry, CLNs were minced between the frosted ends of two glass slides to obtain a single-cell suspension in RPMI-1640 medium (WelGENE) containing 10% FBS (Gibco; Life Technologies). The cells were stained with fluorescence-conjugated anti-mouse antibodies against CD4 (catalog no. 25-0041; eBioscience), FOXP3 (catalog no. 53-5773; eBioscience), IL-17A (catalog no. 560184; BD Biosciences), and IFN-γ (catalog no. 554412; XMG1.2; BD Biosciences), and their isotype control antibodies were used as a negative control. For intracellular staining, the cells were stimulated for 5 hr with 50 ng/mL phorbol myristate acetate and 1 μg/mL ionomycin in the presence of GolgiPlug (BD Pharmingen) and stained. The cells were then assayed for fluorescence using an S1000EXi Flow Cytometer (Stratedigm). Data were analyzed using the Flowjo program (Tree Star).

EV-treated APC phenotypes in the MLR were analyzed by flow cytometry using anti-mouse CD11c (HL3; catalog no. 57400), CD80 (16-10A1; catalog no. 553769), CD86 (GL1; catalog no. 558703), CD40 (3/23; catalog no. 553791), and MHC class II (1-A/1-E; M5/114.15.2; catalog no. 557000) antibodies, and their isotype control antibodies were used as a negative control. All antibodies are from BD Biosciences. A Mouse Treg Detection Kit (Miltenyi Biotec) was used to stain Tregs for flow cytometry analysis.

Real-Time PCR Assay

For molecular assays, the eyeballs were lysed in RNA isolation reagent (RNA Bee; Tel-Test) and homogenized using a sonicator (Ultrasonic Processor; Cole Parmer Instruments). Total RNA was extracted from the eyeballs or splenocyte culture using an RNeasy Mini Kit (QIAGEN), and double-stranded cDNA was synthesized by reverse transcription (High Capacity RNA-to-cDNA Kit; Applied Biosystems; Life Technologies). Real-time PCR amplification (ABI 7900 Sequence

Detector; Applied Biosystems) was performed using TaqMan Universal PCR Master Mix (Applied Biosystems). The PCR probe and primer sets were purchased from Applied Biosystems (TaqMan Gene Expression Assay): *Tnf-α*, *Il-1β*, *Il-2*, *Il-4*, *Il-10*, *Il-6*, *Il-12a*, *Il-17a*, and *Ifn-γ*. For relative quantitation of gene expression, mouse-specific *Gapdh* primers and probe (Mm99999915_g1) were used.

ELISA

Mouse insulin in the plasma from NOD/*scid* mice of the T1D model was detected by a Mouse INSULIN ELISA Kit (EMINS; Thermo Fisher Scientific). Mouse IL-12, IL-10, IFN-γ, IL-2, IL-6, and Th17A/F in the culture supernatants were measured by commercial ELISA kits (R&D Systems) according to the manufacturer's protocol.

SUPPLEMENTAL INFORMATION

Supplemental Information includes two figures and can be found with this article online at http://dx.doi.org/10.1016/j.stemcr.2017.04.008.

AUTHOR CONTRIBUTIONS

T.S.K. and J.Y.O. contributed equally to this work. J.Y.O., D.J.P., and R.H.L. designed the research; T.S.K., J.Y.O., D.K., H.J.J., S.Y.P., H.J.L., J.W.P., S.Y.A., and R.H.L. performed experiments; T.S.K., J.Y.O., T.W.K., and R.H.L. analyzed data; and T.S.K, J.Y.O., and R.H.L. wrote the paper.

ACKNOWLEDGMENTS

This research was supported by the Korea Health Technology R&D Project through the Korea Health Industry Development Institute (KHIDI), funded by the Ministry of Health & Welfare, Republic of Korea (grant number: lHI15C3134); the NIH (grant number: P40RR17447).

Received: October 25, 2016
Revised: April 6, 2017
Accepted: April 7, 2017
Published: May 9, 2017

REFERENCES

Abdi, R., Fiorina, P., Adra, C.N., Atkinson, M., and Sayegh, M.H. (2008). Immunomodulation by mesenchymal stem cells: a potential therapeutic strategy for type 1 diabetes. Diabetes *57*, 1759–1767.

Aggarwal, S., and Pittenger, M.F. (2005). Human mesenchymal stem cells modulate allogeneic immune cell responses. Blood *105*, 1815–1822.

Akiyama, K., Chen, C., Wang, D., Xu, X., Qu, C., Yamaza, T., Cai, T., Chen, W., Sun, L., and Shi, S. (2012). Mesenchymal-stem-cell-induced immunoregulation involves FAS-ligand-/FAS-mediated T cell apoptosis. Cell Stem Cell *10*, 544–555.

Aldinucci, A., Rizzetto, L., Pieri, L., Nosi, D., Romagnoli, P., Biagioli, T., Mazzanti, B., Saccardi, R., Beltrame, L., Massacesi, L., et al. (2010). Inhibition of immune synapse by altered dendritic cell actin distribution: a new pathway of mesenchymal stem cell immune regulation. J. Immunol. *185*, 5102–5110.

Alleva, D.G., Johnson, E.B., Wilson, J., Beller, D.I., and Conlon, P.J. (2001). SJL and NOD macrophages are uniquely characterized by genetically programmed, elevated expression of the IL-12(p40) gene, suggesting a conserved pathway for the induction of organ-specific autoimmunity. J. Leukoc. Biol. *69*, 440–448.

Ankrum, J.A., Ong, J.F., and Karp, J.M. (2014). Mesenchymal stem cells: immune evasive, not immune privileged. Nat. Biotechnol. *32*, 252–260.

Baglio, S.R., Rooijers, K., Koppers-Lalic, D., Verweij, F.J., Perez Lanzon, M., Zini, N., Naaijkens, B., Perut, F., Niessen, H.W., Baldini, N., and Pegtel, D.M. (2015). Human bone marrow- and adipose-mesenchymal stem cells secrete exosomes enriched in distinctive miRNA and tRNA species. Stem Cell Res. Ther. *6*, 127.

Barkholt, L., Flory, E., Jekerle, V., Lucas-Samuel, S., Ahnert, P., Bisset, L., Buscher, D., Fibbe, W., Foussat, A., Kwa, M., et al. (2013). Risk of tumorigenicity in mesenchymal stromal cell-based therapies–bridging scientific observations and regulatory viewpoints. Cytotherapy *15*, 753–759.

Bettelli, E., Oukka, M., and Kuchroo, V.K. (2007). T(H)-17 cells in the circle of immunity and autoimmunity. Nat. Immunol. *8*, 345–350.

Beyth, S., Borovsky, Z., Mevorach, D., Liebergall, M., Gazit, Z., Aslan, H., Galun, E., and Rachmilewitz, J. (2005). Human mesenchymal stem cells alter antigen-presenting cell maturation and induce T-cell unresponsiveness. Blood *105*, 2214–2219.

Boltze, J., Arnold, A., Walczak, P., Jolkkonen, J., Cui, L., and Wagner, D.C. (2015). The dark side of the force - constraints and complications of cell therapies for stroke. Front. Neurol. *6*, 155.

Caspi, R.R. (2003). Experimental autoimmune uveoretinitis in the rat and mouse. Curr. Protoc. Immunol. *Chapter 15*, Unit 15.6.

Chen, J., Li, C., and Chen, L. (2015). The role of microvesicles derived from mesenchymal stem cells in lung diseases. Biomed. Res. Int. *2015*, 985814.

Chiesa, S., Morbelli, S., Morando, S., Massollo, M., Marini, C., Bertoni, A., Frassoni, F., Bartolome, S.T., Sambuceti, G., Traggiai, E., and Uccelli, A. (2011). Mesenchymal stem cells impair in vivo T-cell priming by dendritic cells. Proc. Natl. Acad. Sci. USA *108*, 17384–17389.

Crane, I.J., and Forrester, J.V. (2005). Th1 and Th2 lymphocytes in autoimmune disease. Crit. Rev. Immunol. *25*, 75–102.

Doeppner, T.R., Herz, J., Gorgens, A., Schlechter, J., Ludwig, A.K., Radtke, S., de Miroschedji, K., Horn, P.A., Giebel, B., and Hermann, D.M. (2015). Extracellular vesicles improve post-stroke neuroregeneration and prevent postischemic immunosuppression. Stem Cells Transl. Med. *4*, 1131–1143.

Furlani, D., Ugurlucan, M., Ong, L., Bieback, K., Pittermann, E., Westien, I., Wang, W., Yerebakan, C., Li, W., Gaebel, R., et al. (2009). Is the intravascular administration of mesenchymal stem cells safe? Mesenchymal stem cells and intravital microscopy. Microvasc. Res. *77*, 370–376.

Heldring, N., Mager, I., Wood, M.J., Le Blanc, K., and Andaloussi, S.E. (2015). Therapeutic potential of multipotent mesenchymal

stromal cells and their extracellular vesicles. Hum. Gene Ther. *26*, 506–517.

Heslop, J.A., Hammond, T.G., Santeramo, I., Tort Piella, A., Hopp, I., Zhou, J., Baty, R., Graziano, E.I., Proto Marco, B., Caron, A., et al. (2015). Concise review: workshop review: understanding and assessing the risks of stem cell-based therapies. Stem Cells Transl. Med. *4*, 389–400.

Hood, J.L., San, R.S., and Wickline, S.A. (2011). Exosomes released by melanoma cells prepare sentinel lymph nodes for tumor metastasis. Cancer Res. *71*, 3792–3801.

Isakova, I.A., Lanclos, C., Bruhn, J., Kuroda, M.J., Baker, K.C., Krishnappa, V., and Phinney, D.G. (2014). Allo-reactivity of mesenchymal stem cells in rhesus macaques is dose and haplotype dependent and limits durable cell engraftment in vivo. PLoS One *9*, e87238.

Jain, R., Tartar, D.M., Gregg, R.K., Divekar, R.D., Bell, J.J., Lee, H.H., Yu, P., Ellis, J.S., Hoeman, C.M., Franklin, C.L., and Zaghouani, H. (2008). Innocuous IFNgamma induced by adjuvant-free antigen restores normoglycemia in NOD mice through inhibition of IL-17 production. J. Exp. Med. *205*, 207–218.

Jiang, X.X., Zhang, Y., Liu, B., Zhang, S.X., Wu, Y., Yu, X.D., and Mao, N. (2005). Human mesenchymal stem cells inhibit differentiation and function of monocyte-derived dendritic cells. Blood *105*, 4120–4126.

Jun, H.S., Yoon, C.S., Zbytnuik, L., van Rooijen, N., and Yoon, J.W. (1999). The role of macrophages in T cell-mediated autoimmune diabetes in nonobese diabetic mice. J. Exp. Med. *189*, 347–358.

Jung, J.W., Kwon, M., Choi, J.C., Shin, J.W., Park, I.W., Choi, B.W., and Kim, J.Y. (2013). Familial occurrence of pulmonary embolism after intravenous, adipose tissue-derived stem cell therapy. Yonsei Med. J. *54*, 1293–1296.

Jurewicz, M., Yang, S., Augello, A., Godwin, J.G., Moore, R.F., Azzi, J., Fiorina, P., Atkinson, M., Sayegh, M.H., and Abdi, R. (2010). Congenic mesenchymal stem cell therapy reverses hyperglycemia in experimental type 1 diabetes. Diabetes *59*, 3139–3147.

Kidd, S., Spaeth, E., Dembinski, J.L., Dietrich, M., Watson, K., Klopp, A., Battula, V.L., Weil, M., Andreeff, M., and Marini, F.C. (2009). Direct evidence of mesenchymal stem cell tropism for tumor and wounding microenvironments using in vivo bioluminescent imaging. Stem Cells *27*, 2614–2623.

Kim, D.K., Nishida, H., An, S.Y., Shetty, A.K., Bartosh, T.J., and Prockop, D.J. (2016). Chromatographically isolated CD63+CD81+ extracellular vesicles from mesenchymal stromal cells rescue cognitive impairments after TBI. Proc. Natl. Acad. Sci. USA *113*, 170–175.

Kimura, A., Naka, T., and Kishimoto, T. (2007). IL-6-dependent and -independent pathways in the development of interleukin 17-producing T helper cells. Proc. Natl. Acad. Sci. USA *104*, 12099–12104.

Ko, J.H., Lee, H.J., Jeong, H.J., Kim, M.K., Wee, W.R., Yoon, S.O., Choi, H., Prockop, D.J., and Oh, J.Y. (2016). Mesenchymal stem/stromal cells precondition lung monocytes/macrophages to produce tolerance against allo- and autoimmunity in the eye. Proc. Natl. Acad. Sci. USA *113*, 158–163.

Kota, D.J., Wiggins, L.L., Yoon, N., and Lee, R.H. (2013). TSG-6 produced by hMSCs delays the onset of autoimmune diabetes by suppressing Th1 development and enhancing tolerogenicity. Diabetes *62*, 2048–2058.

Kronsteiner, B., Peterbauer-Scherb, A., Grillari-Voglauer, R., Redl, H., Gabriel, C., van Griensven, M., and Wolbank, S. (2011). Human mesenchymal stem cells and renal tubular epithelial cells differentially influence monocyte-derived dendritic cell differentiation and maturation. Cell. Immunol. *267*, 30–38.

Lai, R.C., Yeo, R.W., Tan, K.H., and Lim, S.K. (2013). Exosomes for drug delivery - a novel application for the mesenchymal stem cell. Biotechnol. Adv. *31*, 543–551.

Langrish, C.L., Chen, Y., Blumenschein, W.M., Mattson, J., Basham, B., Sedgwick, J.D., McClanahan, T., Kastelein, R.A., and Cua, D.J. (2005). IL-23 drives a pathogenic T cell population that induces autoimmune inflammation. J. Exp. Med. *201*, 233–240.

Lee, R.H., Pulin, A.A., Seo, M.J., Kota, D.J., Ylostalo, J., Larson, B.L., Semprun-Prieto, L., Delafontaine, P., and Prockop, D.J. (2009a). Intravenous hMSCs improve myocardial infarction in mice because cells embolized in lung are activated to secrete the anti-inflammatory protein TSG-6. Cell Stem Cell *5*, 54–63.

Lee, R.H., Seo, M.J., Pulin, A.A., Gregory, C.A., Ylostalo, J., and Prockop, D.J. (2009b). The CD34-like protein PODXL and alpha6-integrin (CD49f) identify early progenitor MSCs with increased clonogenicity and migration to infarcted heart in mice. Blood *113*, 816–826.

Lee, R.H., Oh, J.Y., Choi, H., and Bazhanov, N. (2011). Therapeutic factors secreted by mesenchymal stromal cells and tissue repair. J. Cell. Biochem. *112*, 3073–3078.

Lee, R.H., Yu, J.M., Foskett, A.M., Peltier, G., Reneau, J.C., Bazhanov, N., Oh, J.Y., and Prockop, D.J. (2014). TSG-6 as a biomarker to predict efficacy of human mesenchymal stem/progenitor cells (hMSCs) in modulating sterile inflammation in vivo. Proc. Natl. Acad. Sci. USA *111*, 16766–16771.

Lee, H.J., Ko, J.H., Jeong, H.J., Ko, A.Y., Kim, M.K., Wee, W.R., Yoon, S.O., and Oh, J.Y. (2015). Mesenchymal stem/stromal cells protect against autoimmunity via CCL2-dependent recruitment of myeloid-derived suppressor cells. J. Immunol. *194*, 3634–3645.

Lenardo, M., Chan, K.M., Hornung, F., McFarland, H., Siegel, R., Wang, J., and Zheng, L. (1999). Mature T lymphocyte apoptosis–immune regulation in a dynamic and unpredictable antigenic environment. Annu. Rev. Immunol. *17*, 221–253.

Liu, W.H., Liu, J.J., Wu, J., Zhang, L.L., Liu, F., Yin, L., Zhang, M.M., and Yu, B. (2013). Novel mechanism of inhibition of dendritic cells maturation by mesenchymal stem cells via interleukin-10 and the JAK1/STAT3 signaling pathway. PLoS One *8*, e55487.

Meisel, R., Zibert, A., Laryea, M., Gobel, U., Daubener, W., and Dilloo, D. (2004). Human bone marrow stromal cells inhibit allogeneic T-cell responses by indoleamine 2,3-dioxygenase-mediated tryptophan degradation. Blood *103*, 4619–4621.

Monsel, A., Zhu, Y.G., Gudapati, V., Lim, H., and Lee, J.W. (2016). Mesenchymal stem cell derived secretome and extracellular vesicles for acute lung injury and other inflammatory lung diseases. Expert Opin. Biol. Ther. *16*, 859–871.

Nakae, S., Komiyama, Y., Nambu, A., Sudo, K., Iwase, M., Homma, I., Sekikawa, K., Asano, M., and Iwakura, Y. (2002). Antigen-specific T cell sensitization is impaired in IL-17-deficient mice, causing

suppression of allergic cellular and humoral responses. Immunity *17*, 375–387.

Oh, J.Y., Kim, T.W., Jeong, H.J., Lee, H.J., Ryu, J.S., Wee, W.R., Heo, J.W., and Kim, M.K. (2014). Intraperitoneal infusion of mesenchymal stem/stromal cells prevents experimental autoimmune uveitis in mice. Mediators Inflamm. *2014*, 624640.

Ophelders, D.R., Wolfs, T.G., Jellema, R.K., Zwanenburg, A., Andriessen, P., Delhaas, T., Ludwig, A.K., Radtke, S., Peters, V., Janssen, L., et al. (2016). Mesenchymal stromal cell-derived extracellular vesicles protect the fetal brain after hypoxia-ischemia. Stem Cells Transl. Med. *5*, 754–763.

Ortiz, L.A., Gambelli, F., McBride, C., Gaupp, D., Baddoo, M., Kaminski, N., and Phinney, D.G. (2003). Mesenchymal stem cell engraftment in lung is enhanced in response to bleomycin exposure and ameliorates its fibrotic effects. Proc. Natl. Acad. Sci. USA *100*, 8407–8411.

Ouyang, W., Rutz, S., Crellin, N.K., Valdez, P.A., and Hymowitz, S.G. (2011). Regulation and functions of the IL-10 family of cytokines in inflammation and disease. Annu. Rev. Immunol. *29*, 71–109.

Phinney, D.G., Di Giuseppe, M., Njah, J., Sala, E., Shiva, S., St Croix, C.M., Stolz, D.B., Watkins, S.C., Di, Y.P., Leikauf, G.D., et al. (2015). Mesenchymal stem cells use extracellular vesicles to outsource mitophagy and shuttle microRNAs. Nat. Commun. *6*, 8472.

Rafei, M., Hsieh, J., Fortier, S., Li, M., Yuan, S., Birman, E., Forner, K., Boivin, M.N., Doody, K., Tremblay, M., et al. (2008). Mesenchymal stromal cell-derived CCL2 suppresses plasma cell immunoglobulin production via STAT3 inactivation and PAX5 induction. Blood *112*, 4991–4998.

Rani, S., Ryan, A.E., Griffin, M.D., and Ritter, T. (2015). Mesenchymal stem cell-derived extracellular vesicles: toward cell-free therapeutic applications. Mol. Ther. *23*, 812–823.

Rojas, M., Xu, J., Woods, C.R., Mora, A.L., Spears, W., Roman, J., and Brigham, K.L. (2005). Bone marrow-derived mesenchymal stem cells in repair of the injured lung. Am. J. Respir. Cell Mol. Biol. *33*, 145–152.

Sato, K., Ozaki, K., Oh, I., Meguro, A., Hatanaka, K., Nagai, T., Muroi, K., and Ozawa, K. (2007). Nitric oxide plays a critical role in suppression of T-cell proliferation by mesenchymal stem cells. Blood *109*, 228–234.

Spaggiari, G.M., Abdelrazik, H., Becchetti, F., and Moretta, L. (2009). MSCs inhibit monocyte-derived DC maturation and function by selectively interfering with the generation of immature DCs: central role of MSC-derived prostaglandin E2. Blood *113*, 6576–6583.

Tatsumi, K., Ohashi, K., Matsubara, Y., Kohori, A., Ohno, T., Kakidachi, H., Horii, A., Kanegae, K., Utoh, R., Iwata, T., and Okano, T. (2013). Tissue factor triggers procoagulation in transplanted mesenchymal stem cells leading to thromboembolism. Biochem. Biophys. Res. Commun. *431*, 203–209.

Vader, P., Mol, E.A., Pasterkamp, G., and Schiffelers, R.M. (2016). Extracellular vesicles for drug delivery. Adv. Drug Deliv. Rev. *106*, 148–156.

Wang, J., Yoshida, T., Nakaki, F., Hiai, H., Okazaki, T., and Honjo, T. (2005). Establishment of NOD-Pdcd1-/- mice as an efficient animal model of type I diabetes. Proc. Natl. Acad. Sci. USA *102*, 11823–11828.

Weaver, D.J., Jr., Poligone, B., Bui, T., Abdel-Motal, U.M., Baldwin, A.S., Jr., and Tisch, R. (2001). Dendritic cells from nonobese diabetic mice exhibit a defect in NF-kappa B regulation due to a hyperactive I kappa B kinase. J. Immunol. *167*, 1461–1468.

Wei, X., Yang, X., Han, Z.P., Qu, F.F., Shao, L., and Shi, Y.F. (2013). Mesenchymal stem cells: a new trend for cell therapy. Acta Pharmacol. Sin. *34*, 747–754.

Wen, S., Dooner, M., Cheng, Y., Papa, E., Del Tatto, M., Pereira, M., Deng, Y., Goldberg, L., Aliotta, J., Chatterjee, D., et al. (2016). Mesenchymal stromal cell-derived extracellular vesicles rescue radiation damage to murine marrow hematopoietic cells. Leukemia *30*, 2221–2231.

Zhang, W., Ge, W., Li, C., You, S., Liao, L., Han, Q., Deng, W., and Zhao, R.C. (2004). Effects of mesenchymal stem cells on differentiation, maturation, and function of human monocyte-derived dendritic cells. Stem Cells Dev. *13*, 263–271.

Zhang, B., Liu, R., Shi, D., Liu, X., Chen, Y., Dou, X., Zhu, X., Lu, C., Liang, W., Liao, L., et al. (2009). Mesenchymal stem cells induce mature dendritic cells into a novel Jagged-2-dependent regulatory dendritic cell population. Blood *113*, 46–57.

Zhang, H., Wang, Y., Hwang, E.S., and He, Y.W. (2016). Interleukin-10: an immune-activating cytokine in cancer immunotherapy. J. Clin. Oncol. http://dx.doi.org/10.1200/JCO.2016.69.6435.

Stem Cell Reports, Volume *8*

Supplemental Information

MSC-derived Extracellular Vesicles Attenuate Immune Responses in Two Autoimmune Murine Models: Type 1 Diabetes and Uveoretinitis

Taeko Shigemoto-Kuroda, Joo Youn Oh, Dong-ki Kim, Hyun Jeong Jeong, Se Yeon Park, Hyun Ju Lee, Jong Woo Park, Tae Wan Kim, Su Yeon An, Darwin J. Prockop, and Ryang Hwa Lee

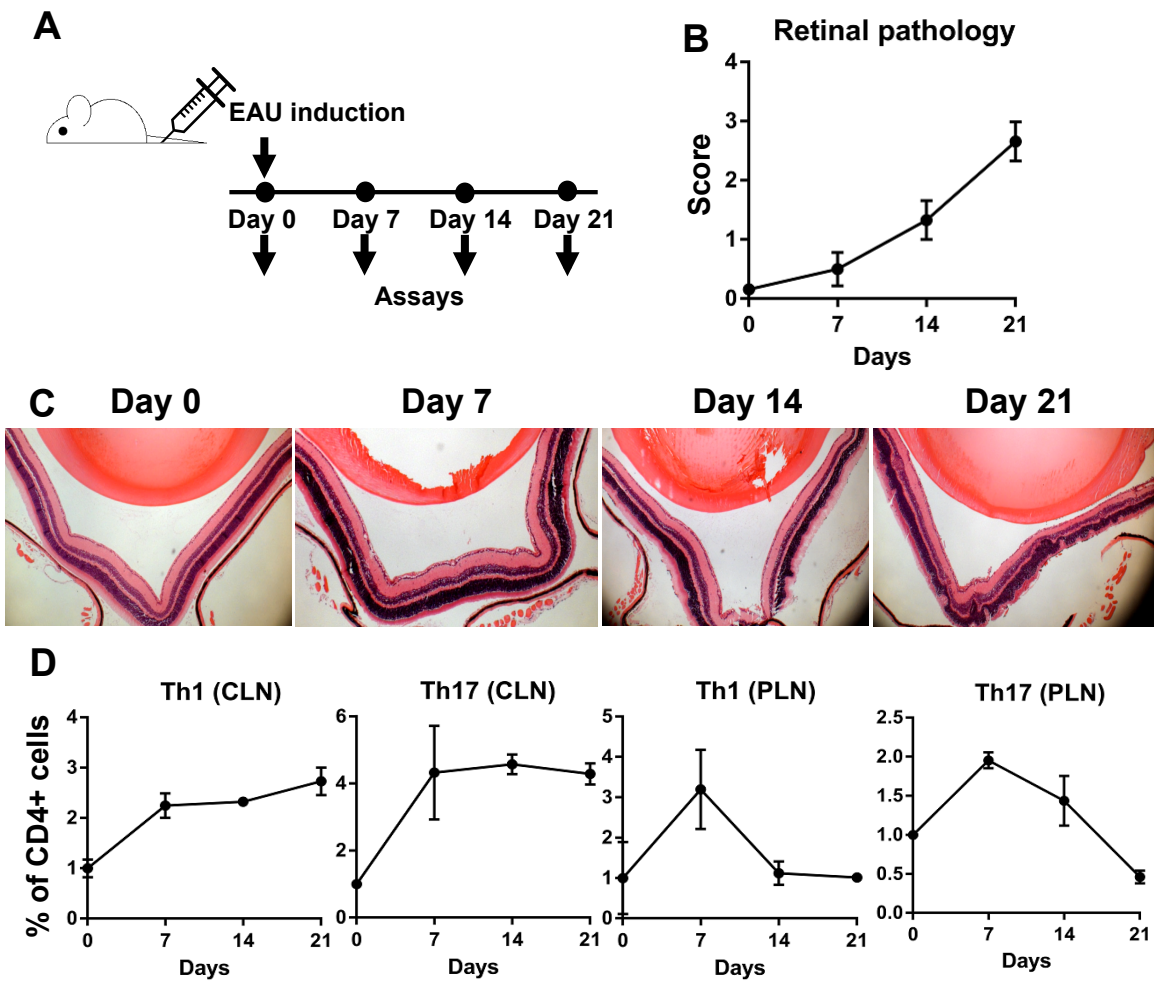

Figure S1. Time course of retinal pathology and the percentages of Th1 and Th17 cells in lymph nodes. (Related to Figure 3)

A. Experimental scheme. On day 0, EAU was induced, and on days 7, 14, and 21, the eyes and lymph nodes were evaluated (n=5 mice per each time point). Retinal pathology scoring (**B**) and representative pictures (**C**) of the retina with time after EAU immunization. **D.** Cytometric analysis of cervical (CLN) and popliteal lymph nodes (PLN) with time after EAU immunization.

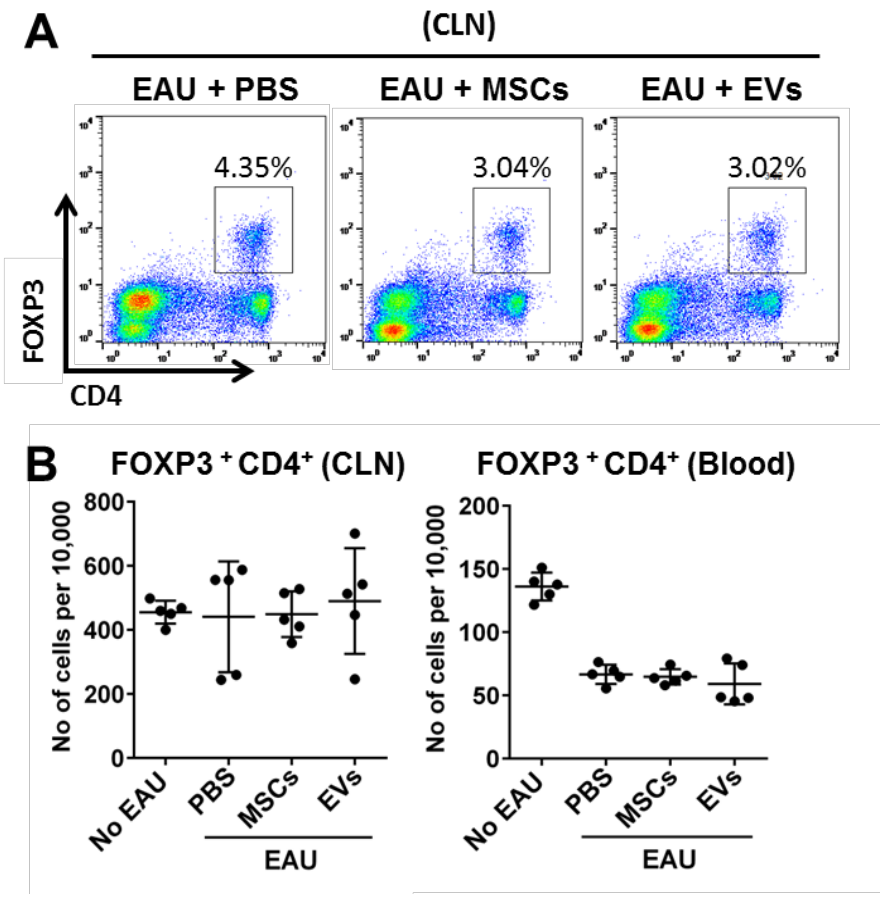

Figure S2. Treg analysis in cervical lymph nodes and blood of mice treated with MSCs or EVs. (Related to Figure 4)

Representative flow cytometry plots (**A**) and quantitative results (**B**) for $FOXP3^{+}CD4^{+}$ Tregs in cervical lymph nodes (CLNs) and peripheral blood collected from EAU mice treated with PBS, MSCs, or EVs. For controls, normal mice without EAU induction were used. Dot indicates a single animal (n=5 per each group).